FILM-DROPLET SPLIT CORRELATION AT THE ONSET OF ANNULAR-MIST FLOW

S. Oh*, B. Hizoum, P. Saha, B. Dooies, D. Miranda
GE Hitachi Nuclear Energy
3901 Castle Hayne Road, M/C A55
Wilmington, NC 28401, USA
seungmin1.oh@gnf.com; belgacem.hizoum@gnf.com; pradip.saha@ge.com;
brett.dooies@ge.com; dana.miranda@ge.com

J. G. M. Andersen
Consultant
jandersen@ec.rr.com

ABSTRACT

Boiling transition in BWR fuels occurs in the annular-mist flow regime. Many subchannel analysis methods have been developed to predict critical power, as well as flow and void distributions, in BWR fuel bundles. Two-phase annular-mist flow can be better simulated with two-fluid, three-field formulations for liquid film flow on surfaces, vapor and entrained droplet flows inside the core of the subchannel. To predict dryout of BWR fuels in the annular flow regime, the liquid film mass balance is analyzed using appropriate droplet entrainment and deposition models along with evaporation to determine the condition when film dries out or a dry patch forms (i.e. boiling transition). It is of great importance to define a correct boundary condition for the liquid flow split between the liquid film and entrained droplets at the onset of annular flow to accurately model the entrainment and deposition at the downstream annular flow, predict dryout location and corresponding critical power. No reliable information on the film-droplet split at onset of annular flow have been found in the literature and most analyses have been performed with an assumption that a single value is valid for wide ranges of operating conditions. In this study, a new film-droplet split correlation in the form of film fraction is developed based on available data with steam-water experiments. The liquid split correlation is then applied to simulate film flow measurement data over a wide range of exit quality.

KEYWORDS
Boiling transition, annular flow, subchannel analysis, film-droplet split, entrainment

1. INTRODUCTION

GE Hitachi Nuclear Energy (GEH) has developed a detailed subchannel analysis code COBRAG [1] with the main objective of predicting critical power, bundle pressure drop and void distributions in BWR fuel bundles. The two-phase flow is described by conservation equations derived from a two-fluid (e.g. liquid and vapor), multi-field (e.g. continuous, dispersed and multi-film) model. This model, which simulates liquid films on unique surfaces within a subchannel as having their own set of conservation equations, proves to be crucial in predicting dryout or the onset of boiling transition (BT). The conservation

* Corresponding Author

equations are then coupled with other physical models/correlations, or constitutive relations, for the wall and interfacial shear, interfacial heat transfer, liquid entrainment and deposition rates, inter-subchannel mixing, and void drift for closure.

COBRAG predictions [1] for entrainment fraction (F_{ENT}) in annular flow, defined as the ratio of droplet flow to the sum of droplet and film flow, from simple geometry experiments conducted at Risø [2] showed a need for further improvement of the entrainment and deposition rate models. A set of equilibrium entrainment and deposition rate models was developed [3] using the Risø data, which were collected from high-pressure, high-temperature steam-water adiabatic experiments in round tube and annulus geometry. Application of this set of equilibrium entrainment/deposition rate models to the heated tests conducted in a shorter test section with heights that are prototypical of a BWR fuel assembly showed that the correct split of total liquid in forms of film and droplets at the onset of annular-mist flow regime was also important to obtain a good prediction of film flow rates and entrainment fractions [3].

Dryout of BWR fuels in annular flow is predicted by a liquid film mass balance using appropriate droplet entrainment and deposition models along with evaporation. It is of great importance to define a correct boundary condition for the liquid flow split between the liquid film and entrained droplets at the onset of annular flow. However, it is difficult to obtain good experimental data at the onset of annular flow due to the complicated nature of the flow structure at the boundary of churn-turbulent flow and annular flow. As a result, limited information relevant to the film-droplet split has been available to the two-phase flow community and many researchers have used either a single assumed value of the entrainment fraction at the onset of annular flow or an entrainment model developed from adiabatic equilibrium conditions.

Saito et al. [4] assumed an entrainment fraction of 0.9 at the onset of annular flow while Hewitt and Govan [5] assumed 0.99 as the entrainment fraction at the onset of annular flow.

Barbosa Jr. et al. [6] developed an empirical correlation for the entrainment fraction at the onset of annular flow based on low pressure adiabatic air-water experiments in a vertical test section. This correlation, as shown in Eq. (1), is only applicable to low pressure and doesn't predict well the entrainment fraction of high pressure steam-water data of interest. However, it is worthwhile to note that the entrainment fraction at the onset of annular flow may be expressed as a function of vapor mass flux, liquid mass flux, and hydraulic diameter.

$$F_{ENT} \equiv \frac{W_e}{W_e+W_f} = 0.0095 + 3.4255 \cdot \sqrt{G_L/G_g} \cdot D_h^2 \quad (1)$$

Ahmad et al. [7] assumed a value of 0.7 entrained fraction at the onset of annular flow admitting that the value for the entrainment fraction is important and needs further evaluation. They noted that the predicted dryout location varies little, irrespective of the entrained fraction assumed at the onset of annular flow, in low mass flux cases. However, the predicted position was found to be sensitive to the entrained mass fraction assumed at higher mass flux conditions.

Ahmad et al. [8] tried to start the film flow analysis from the onset of churn flow rather than from the annular flow. This approach is followed by Wang et al. [9] and they argued that droplets with large momentum in churn flow may travel along the flow regime transition into annular flow and affect the downstream flow field. Based on the experimental observation, the entrained fraction at the onset of the churn flow is assumed to be 0.9 by Wang et al. [9]

Dasgupta et al. [10] proposed a model to estimate the film-droplet split at onset of annular flow. The model was based on a force balance on film flow, where the film flow rate is a function of film thickness

and pressure gradient. However, this model has not been validated against measured data at the onset of annular flow.

In this paper, a film-droplet split correlation in the form of film fraction at the onset of annular flow is developed using both adiabatic and diabatic data obtained from geometric and fluid conditions similar to those in modern BWR fuels.

2. FILM-DROPLET SPLIT AT THE ONSET OF ANNULAR FLOW

A new correlation is developed for the film fraction at the onset of annular flow based on high pressure steam-water experimental data. Exact data at the onset of annular flow is difficult to collect due to the complex nature of churn-to-annular flow transition. However, a reasonable database is generated in Risø National Laboratory in Denmark [2]. This section will describe the development process of the new correlation.

2.1. Risø Test Data

Film flow rates, pressure gradients, film thicknesses, wave frequencies and velocities, and dryout heat fluxes were measured in one annular (17 mm ID/26 mm OD) and two tubular test sections (10 and 20 mm ID) with different lengths [2]. Experiments were performed with steam-water two-phase mixtures at pressures ranging from 3 MPa to 9 MPa under adiabatic and diabatic conditions. A wide range of exit vapor quality (0.02 – 0.8) was tested. A summary of Risø test conditions with liquid film flow measurements is provided in Table 1. The film flow measurements were conducted by extraction of the film through a permeable section at the exit of test section.

Table 1. Risø Test Conditions

Data Series	100	200	300	500	600
Test Section	Annulus	Tube	Tube	Annulus	Tube
Diameter, mm	17 OD/26 ID	10 ID	10 ID	17 OD/26 ID	20 ID
Heated Length, m	3.5	0	2-6	0	0
Unheated Length, m	0.1	9	0.1-2.0	8	9
Pressure, MPa	7	3-9	3-9	3-9	7
Mass flux, kg/s-m^2	500-1000	500-3000	500-3000	400-2000	500-2000
Exit quality	0.02-0.6	0.08-0.6	0.16-0.8	0.15-0.6	0.2-0.7
Heat flux, MW/m^2	0-1.0	N/A	0.5-1.5	N/A	N/A

A cross-sectional schematic of the Risø test sections is shown in Fig. 1, where red and blue surfaces represent heated and unheated surfaces, respectively. It is noted that the annulus test section had the ability to control heat input to both the inner rod and the outer tube so it can simulate representative subchannels in modern BWR fuels. For example,

- the annulus test section with inner rod heated, test section d) in Fig. 1, simulates a typical corner and edge subchannel Types a) and b) in Fig. 2: an outer colder surface with an inner hot surface,
- the annulus with both surface heated, test section f) in Fig. 1, represents a typical interior subchannel Type c) in Fig. 2: a subchannel surrounded by hot surfaces,

- the annulus test section with the outer tube heated, test section e) in Fig. 1, is similar to typical subchannels next to a large water rod or water box as shown in Types d) and e) in Fig. 2,
- in addition, the large diameter test section c) in Fig. 1 with a 20 mm ID tube represents an open area inside a BWR fuel bundle such as subchannels in partial-length rod/vanished region near a water rod, where the hydraulic diameter is large but heat input is small.

2.2. Film-Droplet Split Correlation

The Wallis correlation for the slug-annular transition (Eq. 11.109 of [11]) suggests that at BWR operating pressure the annular transition would occur in the quality range of 0.12 to 0.16. Among Risø test data in Table 1, data collected at conditions representative of annular transition in BWR fuel bundles are used to develop the film-droplet split correlation at the onset of annular flow.

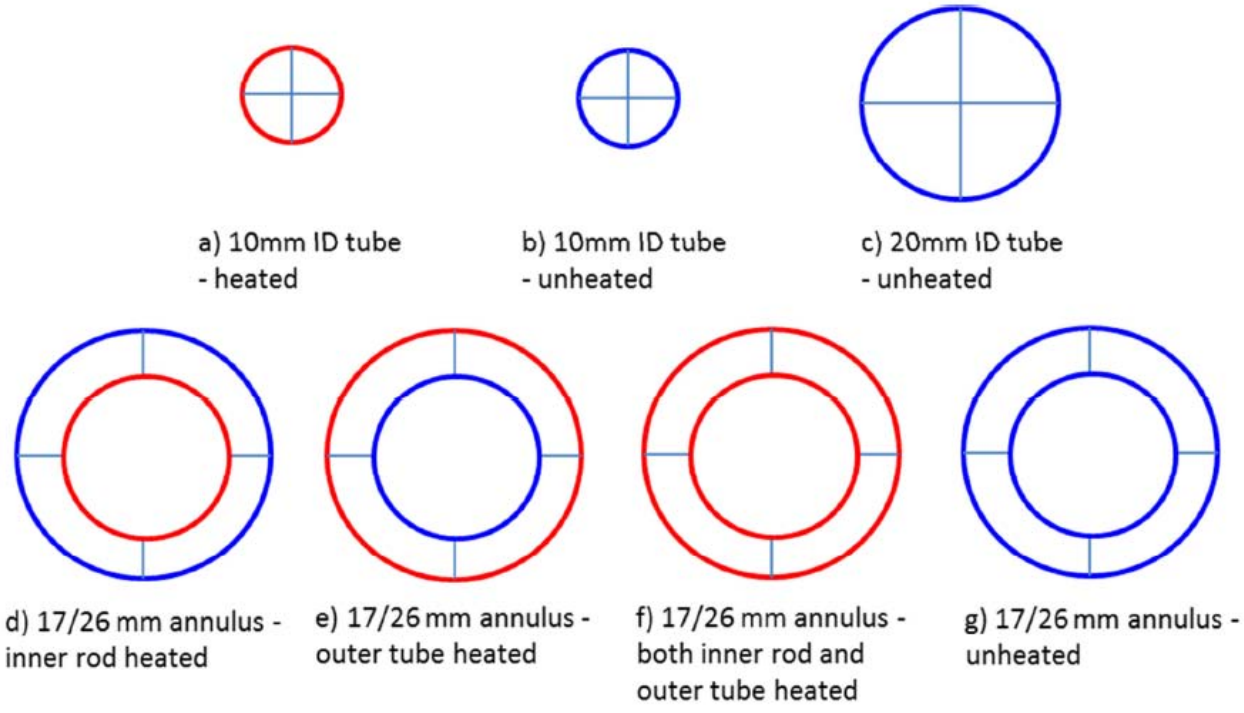

Figure 1. Cross-sectional Schematic of Risø Test Tubes and Annulus

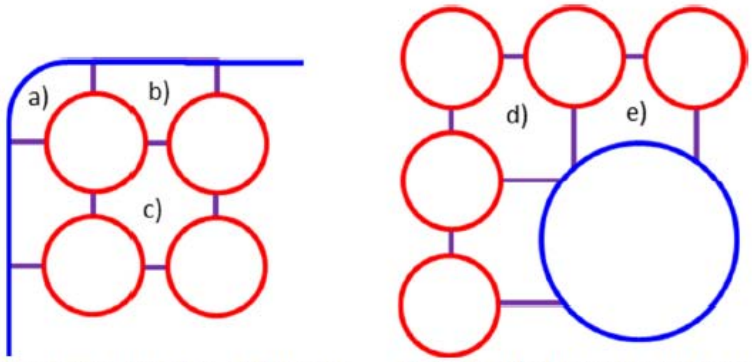

a) corner, b) edge, c) interior, d) & e) subchannels next to water rod

Figure 2. Typical Subchannel Types in Modern BWR Fuels

The entrainment fraction (F_{ENT}) in annular flow is defined as the ratio of droplet flow to the sum of droplet and film flow. For simplicity of data presentation, a new parameter, film fraction or fraction of film flow relative to total liquid flow, is defined as

$$F_{film} = 1 - F_{ENT} = W_f/(W_e + W_f) \quad (2)$$

This should not be confused with the film mass flow fraction (X_f) presented in Figs. 5 and 6, which is the ratio of film to the total mass flow including vapor, film, and droplet flows. Fig. 3 displays the film fraction calculated from the Risø data representing typical conditions at the onset of annular flow in BWR fuel bundles. Several observations can be made from this figure: 1) the film fraction has a strong flow dependence - as flow increases less film or more entrained droplet is available near the onset of annular flow and 2) the geometry of the test section has an effect on the film fraction – as the hydraulic diameter increases, less film and more entrained droplets are available near the onset of annular flow. Forty six (46) data points in Fig. 3 cover a wide range of flow, pressure, geometry, and heat flux conditions similar to BWR fuels at operating conditions.

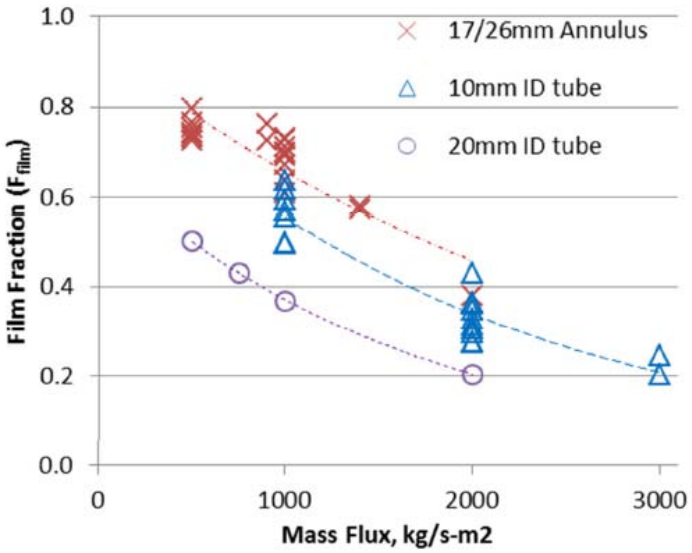

Figure 3. Measured Film Fraction with Mass Flux

A regression analysis on the data reveals that the film fraction data can be well represented with a single parameter, the total Reynolds number, as shown in Fig. 4. The total Reynolds number is defined with the total flow rate and liquid viscosity. The film fraction correlation has lower and upper limit of 0.2 and 0.8, respectively, corresponding to the range of the data utilized:

$$F_{film} = max[0.2, min\{0.8, exp(-0.5 \cdot Re_{TOT}/100{,}000)\}] \quad (3)$$

Where,

$$Re_{TOT} = G_{TOT} \cdot D_h/\mu_L \quad (4)$$

The ranges of database used for the correlation development are: 3 ≤ Pressure (in MPa) ≤ 9, 38,000 ≤ Re_{TOT} ≤ 426,000, 9 < D_h (in mm) ≤ 20. Due to the dimensionless form of the correlation, it can be applied

to a wide range of conditions beyond the ranges of the development database. However, special attention should be paid when the correlation is applied to ranges outside of the development database. The root mean square (RMS) error of the correlation against 46 data points used for the correlation development is 0.065. It is interesting to note that a) the proposed film-droplet split correlation in Eqs. (3) and (4) contains all parameters, either explicitly or implicitly, used in the entrainment fraction correlation in Eq. (1) at the onset of annular flow developed by Barbosa Jr. et al. [6] - vapor mass flux, liquid mass flux, and hydraulic diameter and b) the correlation is also consistent with many equilibrium entrainment correlations that typically predict increased entrainment fractions or reduced film fractions with increasing flow.

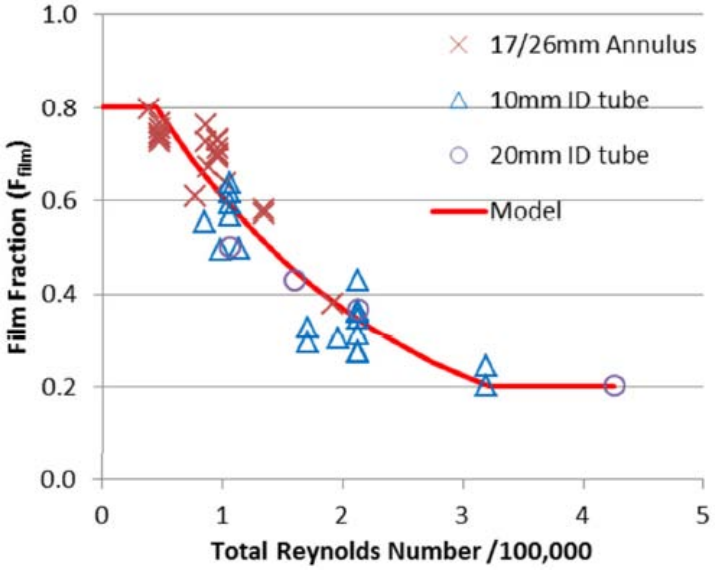

Figure 4. Film Fraction Correlation with Total Reynolds Number

3. COBRAG SIMULATION FOR RISØ HEATED ANNULUS/TUBE DATA

The film-droplet split correlation developed in Section 2 is implemented in the subchannel analysis code, COBRAG [1, 3]. Since shear and heat transfer at vapor–liquid interfaces and wall surfaces vary among flow regimes, COBRAG utilizes a flow regime map (Table 2) for determining these quantities. The flow regime map utilized in COBRAG is divided into two major flow regimes: (a) the liquid continuous flow regime at lower void fractions and (b) the vapor continuous flow regime at higher void fractions with a transition zone in between. The liquid continuous flow regime includes single–phase liquid flow and bubbly/churn flow and is modeled using a two-field model (continuous liquid and dispersed vapor or bubbles). The vapor continuous flow regime includes dispersed annular flow and single–phase vapor flow. The dispersed annular flow is modeled using a three-field model (liquid film on the wall, dispersed droplets in the vapor, and the continuous vapor). For a smooth numerical transition from the two-field model to the three-field model, a fictitious film flow on the wall is formed and computed by initiating the film-droplet split starting at void fraction of 0.3, i.e., the onset of slug-churn or churn flow regime. The COBRAG criterion for the onset of the annular flow is when the liquid in the film can be lifted by the vapor flow [12, 13]. At the first annular flow node in COBRAG, the film flow and droplet flow in each subchannel are determined in such a way that the film fraction calculated by Equation (3) is achieved.

Table 2. COBRAG Flow Regime Map

Void Fraction	Flow Regime
0.0	Single Phase Liquid
$0.0 < \alpha_g < 0.3$	Bubbly Flow
$0.3 < \alpha_g < \alpha_{tran} - 0.1$	Churn Flow
$\alpha_{tran} - 0.1 < \alpha_g < \alpha_{tran}$	Transition Regime
$\alpha_{tran} < \alpha_g < 1.0$	Dispersed Annular Flow
1.0	Single Phase Vapor

3.1. Comparison of Film Mass Flow Fraction

Liquid films were extracted from both the inner rod and outer tube of the annulus at the exit [2]. The film mass flow fraction (X_f) for the inner rod, the outer tube, and the sum of rod and tube calculated from measurement data for the heated annulus test section are compared to COBRAG predictions in Fig. 5. Data points in Fig. 5 span a mass flux range of 500-1000 kg/s-m^2, exit quality of 0.2-0.6, surface heat flux of 0-1.0 MW/m^2 at a pressure of 7 MPa. As shown in Fig. 5, COBRAG tends to over-predict film flows for inner rod and under-predict film flows for outer tube while it predicts well the total film flow (i.e. sum of both inner and outer film). It is believed that the curvature of the surface in the annulus geometry plays a role; i.e., a concave surface of the outer tube attracts more film than a convex surface of the inner rod. However, this characteristic isn't captured in the COBRAG model at the moment. Instead, the total film mass fraction is used as a figure of merit to judge the adequacy of the COBRAG model and the comparison is satisfactory as shown in Fig. 5. In BWR fuel bundles, the curvature effect on the film flow is not expected to be as pronounced as observed in the Risø annulus geometry, where a convex surface and a concave surface face each other. The only surfaces of potential concerns and close to the annulus geometry would be surfaces in the corner subchannel, see Type a) in Fig. 2.

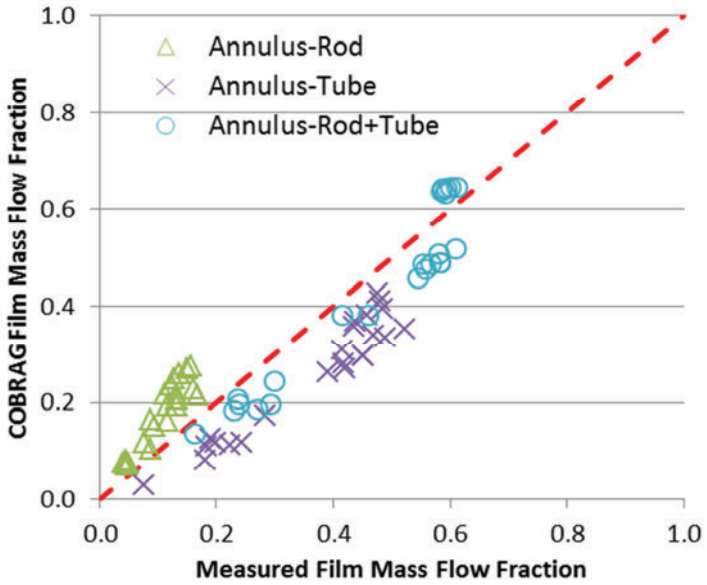

Figure 5. COBRAG Predicted Film Mass Flow Fraction for Heated Annular Test Section

Fig.6 shows a comparison of COBRAG predicted film mass flow fractions for both the annulus and the 10 mm ID heated tube data. Here, the tube data are divided into two categories: with a long (0.5-2.0 m) adiabatic section downstream of the heated section and a standard (0.1 m) adiabatic section. The heated annulus test had the standard adiabatic section of 0.1 m. It is seen from Fig. 6 that the film mass flow fraction error predicted by COBRAG is relatively large for some of the tube data with the long adiabatic section, which suggests that entrainment and deposition models in COBRAG could be improved for the developing region from heated to unheated section. The majority of predictions, however, is within +/- 0.1 and considered satisfactory. It should also be noted that COBRAG tends to under-predict the film flow on the tube data (concave surface) as discussed before. It is believed that the error would be reduced for BWR fuel bundles because the surface curvature effect is much less than the Risø annulus geometry and only the corner subchannel in the BWR fuels would be considerably affected. Fig. 7 presents a comparison of COBRAG predicted entrainment fractions, a more general figure of merit in the literature, for the same data in Fig. 6. The prediction of entrainment fraction is excellent overall for the wide range of data as shown in Fig. 7 and most of the relatively large error cases are for the tube tests with the longer adiabatic section downstream of the heated section. Statistics of delta-entrainment fraction (COBRAG predicted – Data) are summarized in Table 3. It is noted that more bias is observed for the tube data due to the concave surface. Statistics with and without the longer adiabatic tube section downstream of the heated section are reported. Those without the longer adiabatic section are more relevant to the dispersed annular flow region of BWR fuel bundles. As mentioned before, entrainment and deposition rate models applicable to the developing region from heated to unheated section in COBRG could be adjusted to better predict the measured entrainment fraction with longer adiabatic section because the entrainment and deposition rate models play more important roles than the initial film-droplet split correlation for conditions with the longer adiabatic section.

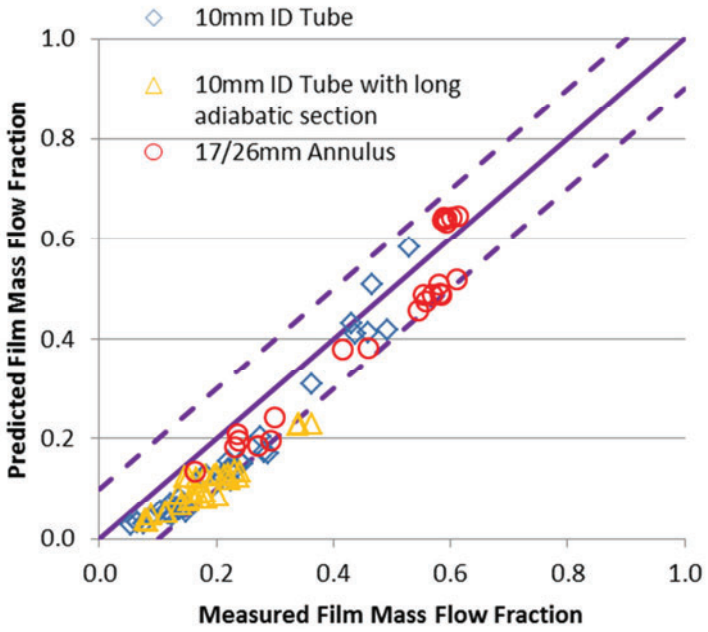

Figure 6. COBRAG Predicted Film Mass Flow Fraction for Heated Annulus/Tube Data

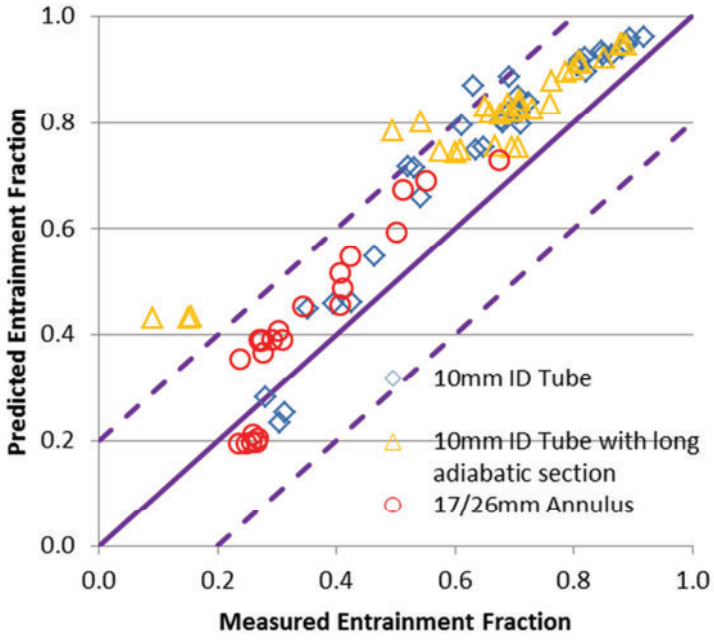

Figure 7. COBRAG Predicted Entrainment Fraction for Heated Annulus/Tube Data

Table 3. Statistics of Delta-Entrainment Fraction (COBRAG predicted – Data) for Heated Annulus/Tube Data

	0.1 m adiabatic section			Tube with long adiabatic section	All
	Annulus	Tube	Subtotal		
Mean Bias	0.063	0.095	**0.082**	0.140	**0.102**
Standard Deviation	0.076	0.064	**0.070**	0.077	**0.077**
No of Data	23	35	**58**	30	**88**

3.2. Axial Development of Film and Droplet Flow Predicted by COBRAG

In this section, detailed COBRAG results for axial development of film and droplet flow and a comparison to measured data are presented for one annulus and one tube data. Test conditions of the two cases are summarized in Table 4.

Table 4. Risø Test Cases for Detailed Comparison

Case	P, bar	Mass Flux, kg/s-m^2	Heat flux @rod, MW/m^2	Heat flux @tube, MW/m^2	Exit quality	Hydraulic diameter, m	Diabatic length, m	Adiabatic length, m
Annulus 107	70	600	0.4	0.4	0.6	0.009	3.5	0.1
Tube 363	70	1000	N/A	1.0	0.6	0.01	4.0	1.0

COBRAG predicted mass flow fractions for vapor, film, and droplet are plotted as a function of axial node in Figures 8 and 9. Measured film and droplet mass flow fractions at the exit are also marked for comparison. For these two cases, the exit vapor mass flow fraction (or vapor quality) is 0.6. The annulus data 107 is selected to show a typical case of good agreement between COBRAG and the film flow data, while the tube data 363 is selected to show a typical case of relatively poor agreement.

For annulus data 107 in Fig. 8, the same heat flux is applied on both the inner rod and outer tube. Churn flow (see Table 2) initiates at node 8 and a fictitious film flow is initiated at this node for numerical smoothing. Then, the annular transition regime starts at node 12 and the full annular flow is achieved at node 15. The heated section extends up to node 36 and node 37 represents the adiabatic section of 0.1 m. COBRAG predicts the exit film and droplet mass flow fraction well as shown in Fig. 8. It is noted that 1) the liquid is not in the droplet form and 2) the liquid film doesn't exist upstream of node 12 (up to Churn flow); physically tangible film and droplet flows can exist from the transition regime or from the annular regime in a more strict sense (node 12 or 15 for this specific case). For simplicity of presentation, droplet flow and film flow up to the Churn flow regime are meant for the continuous liquid flow and the fictitious film flow, respectively, for the purpose of establishing a smooth transition from the two-field model to the three field model. Figs 8 and 9 show how the film-droplet split correlation acts from the Churn flow to the onset of annular flow.

For the 10mm ID tube case with 1.0 m adiabatic section in Fig. 9, the onset of the Churn/Transition/ Annular flow occurs at node 20/23/26, respectively. The heated section extends up to node 41 and node 51 represents the exit of the 1.0 m adiabatic section. For this specific case, COBRAG over-predicts droplet flow at node 51, which means either more entrainment or less deposition or both.

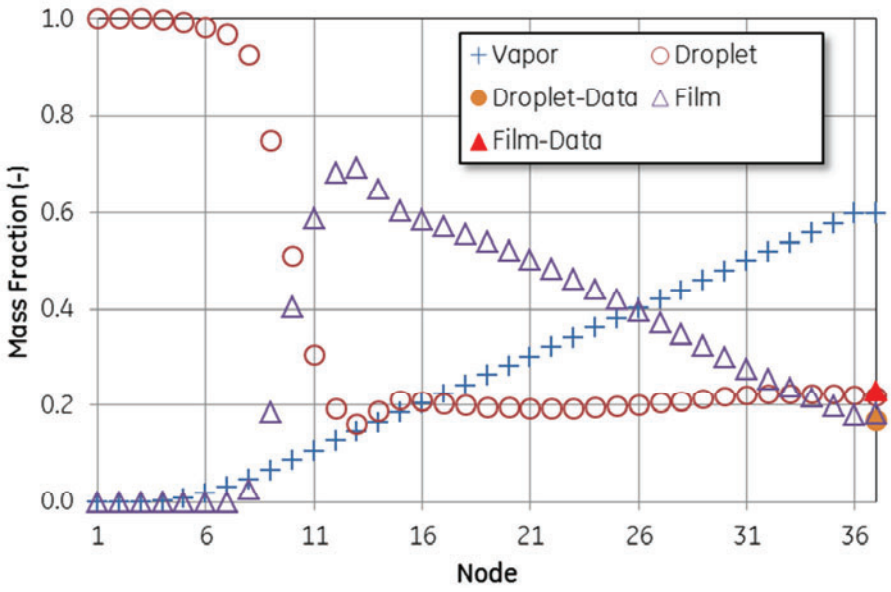

Figure 8. COBRAG Prediction for Annulus data 107

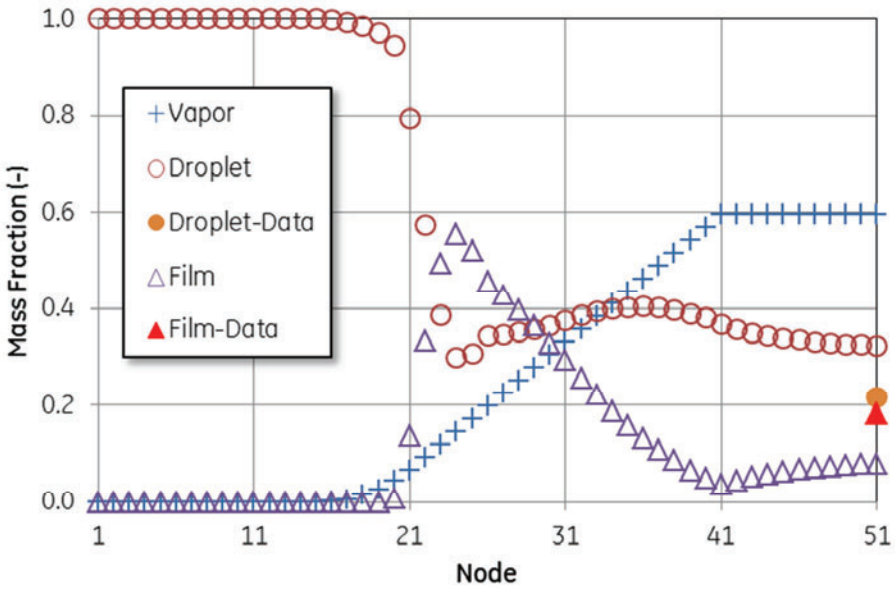

Figure 9. COBRAG Prediction for 10mm Tube data 363

4. CONCLUSIONS AND FUTURE WORK

Subchannel analysis codes have played an important role in predicting detailed void/flow distribution in BWR fuel bundles and are employed in evaluating the onset of boiling transition and critical power. Boiling transition in BWR fuels occurs in the annular-mist flow regime and an accurate flow split between film on surfaces and droplet in vapor core at the onset of annular-mist flow is important to the fidelity of the prediction. A new film-droplet split correlation at the onset of annular flow is developed from high pressure steam-water data. Data used for the correlation development represent conditions typical of annular transition in BWR fuel bundles. The correlation is implemented in the subchannel analysis code, COBRAG.

Then, COBRAG is used to predict film flow measurement data for a wide range of flow quality conditions obtained from heated annulus (both inner rod and outer tube heated) and 10 mm ID heated tube experiments. It is found from comparison to the annulus data that COBRAG under-predicts film flow inside surface of the tube and over-predicts film flow outside surface of the rod: A concave surface of the outer tube attracts more film flow and a convex surface of the inner rod attracts less film flow. The new correlation, however, predicts the overall or total film flow rate well. Statistics of delta-entrainment fraction showed a good agreement with the data. More bias is observed for single tube data compared to the annulus data and it is attributed to the dominant geometric feature (concavity) of the single tube. Less bias is expected for the BWR fuel bundle geometry because the strong effect of surface curvature in the single tube and annulus geometry is diminished in the bundle geometry.

The new correlation better predicts the initial conditions at the onset of annular flow and improves the prediction of film dryout or the onset of boiling transition in BWR fuels. It is also expected to promote more mechanistic constitutive models and less tuning in the subchannel analysis methodology.

The proposed correlation is applied to predict the film flow rates measured at the exit of various Risø test sections [2], and reasonable agreement is found. Further validation against other available data for axial development of film flow is recommended as future work.

NOMENCLATURE

W = mass flow rate; $W_g+W_e+W_f = W_{TOT}$
G = mass flux = mass flux rate / total flow area; $G_g+G_e+G_f = G_{TOT} = W_{TOT} / A_{TOT}$
A = flow area; $A_g+A_e+A_f = A_{TOT}$
D_h= hydraulic diameter
Re = Reynolds number
X_i = mass flow fraction for i (i=g, e, f) = W_i/W_{TOT}, $X_g+X_e+X_f = 1$
F_{ENT} = entrainment fraction = $W_e/(W_e+W_f)$
F_{film} = film fraction = 1 - F_{ENT} = $W_f/(W_e+W_f)$
α = void fraction
μ_L= dynamic viscosity for liquid

Subscript
TOT = total
L = liquid including entrained droplet and liquid film
g = vapor
e = entrained droplet
f = liquid film

REFERENCES

1. B. Hizoum, J. Andersen, A. Sakouda and S. Bowman, "COBRAG Subchannel Analysis of BWR Fuel Thermal Hydraulic Performance," *2010 LWR Fuel Performance/TopFuel/WRFPM*, Orlando, Florida, USA, September 26-29, 2010, pp. 668-680 (2010).
2. J. Würtz, "*An Experimental and Theoretical Investigation of Annular Steam-Water Flow in Tubes and Annuli at 30 to 90 bar*," Risø National Laboratory Report No. 372, Denmark (1978).
3. B. Hizoum, P. Saha, J.G.M. Andersen, and K. Whitelow, "Droplet Entrainment and Deposition Rate Models for determination of Boiling Transition in BWR Fuel Assembly," *14th Int. Topical Meeting on Nuclear Reactor Thermal Hydraulics*, Toronto, Ontario, Canada, Paper No. 387 (2011).
4. T. Saito, E.D. Hughes, M.W. Carbon, "Multi-fluid modelling of annular two-phase flow," *Nucl. Eng. Des.*, **50**, pp 225-271 (1978).
5. G.F. Hewitt, A.H. Govan, "Phenomenological modelling of non-equilibrium flows with phase change," *Int. J. Heat Mass Trans*, **33**, pp. 229-242 (1990).
6. J.R. Barbosa Jr., G.F. Hewitt, G. König, S.M. Richardson, "Liquid entrainment, droplet concentration and pressure gradient at the onset of annular flow in a vertical pipe," *Int. J. Multiphase Flow*, **28**, pp. 943-961 (2002).
7. M. Ahmad, D.K. Chandraker, G.F. Hewitt, P.K. Vijayan, S.P. Walker, "Phenomenological modeling of critical heat flux: The GRAMP code and its validation," *Nucl. Eng. Deg.*, **254**, pp 280-290 (2013).
8. M. Ahmad, D.J. Peng, C.P. Hale, S.P. Walker, G.F. Hewitt, "Droplet entrainment in churn flow," 7th International Conference of Multiphase Flow (ICMF 2010), Florida, USA (2010).
9. K. Wang, B. Bai, W. Ma, "An improved liquid film model to predict the CHF based on the influence of churn flow," *Applied Thermal Engineering*, **64**, pp 422-429 (2014).
10. A. Dasgupta, D.K. Chandraker, A.K. Vishnoi, P.K. Vijayan, "A new methodology for estimation of initial entrainment fraction in annular flow for improved dryout prediction," *Annals of Nuclear Energy*, **75**, pp. 323-330 (2015).
11. G. B. Wallis, "*One-dimensional Two-phase Flow*," McGraw-Hill Book Company (1969).
12. M. Ishii, "*One Dimensional Drift–Flux Model and Constitutive Equations for Relative Motion Between Phases in Various Two–Phase Flow Regimes*", ANL–77–47 (1977).
13. Y. Taitel, D. Borvea and A. E. Dukler, "Modeling Flow Pattern Transitions for Steady Upward Gas–Liquid Flow in Vertical Tubes", *AIChE Journal*, No. 3, pp. 345–354 (1980).